

Preparation and characterization of Ag₂CrO₄/few layer boron nitride hybrids for visible-light-driven photocatalysis

Xiang-feng Wu · Ze-hua Zhao · Yang Sun · Hui Li ·
Chen-xu Zhang · Yi-jin Wang · Yu Liu ·
Yu-duan Wang · Xin-yue Yang · Xiao-dong Gong

Received: 28 January 2017 / Accepted: 11 May 2017 / Published online: 30 May 2017
© Springer Science+Business Media Dordrecht 2017

Abstract Nanosized Ag₂CrO₄/few layer boron nitride composites were prepared via in situ precipitation method. The crystal structure, morphology, optical properties, and charge carrier behavior were investigated by X-ray diffraction, transmission electrical microscopy, UV-vis diffuse reflectance spectroscopy, and electrochemical impedance spectroscopy, respectively. The photocatalytic activities of the as-prepared hybrids were discussed by degradation of rhodamine B under visible-light irradiation. Experimental results showed that the average size of pure Ag₂CrO₄ particles was about 20 nm. Moreover, the degradation efficiency of the as-prepared hybrids was first increased and then decreased with increasing the usage amount of few layer boron nitride nanosheets. When it was 10 wt%, in 120 min, the degradation efficiency of the as-prepared hybrids had reached the maximum of 96.7%. It was much higher than 75% of pure Ag₂CrO₄ nanoparticles. After 3 cycles of the degradation, the efficiency of the as-prepared composites was decreased from 96.7 to 91.8%. Trapping experiment results revealed that holes played a major role during the photocatalysis process. In addition, electrochemical impedance spectroscopy results indicated that few layer boron nitride nanosheets could enhance the separation and transfer of photogenerated electrons and holes.

Keywords Silver chromate · Boron nitride nanosheets · Rhodamine B · Photocatalytic activity · Nanostructured catalysts · Nanocomposite catalysts

Introduction

In the past decades, environmental problem in many countries becomes more and more serious due to the industrialization, population growth, emission of poisonous pollutants, and so on (Tong et al. 2012; Pirhashemi and Habibi-Yangjeh 2015). Recently, many semiconductors, such as TiO₂ (Wandre et al. 2015), ZnO (Peng et al. 2013), and Zn₂SnO₄ (Mali et al. 2015), can be activated under the UV irradiation. However, those visible-light-driven photocatalysts, such as AgBr (Zhao et al. 2016), Ag₃VO₄ (Pirhashemi and Habibi-Yangjeh 2016a, b), Ag₂CrO₄ (Pirhashemi and Habibi-Yangjeh 2016a, b), and Ag₂SO₄ (Cao et al. 2015), have drawn much attentions due to their wide absorption range under the visible light. They can be used as the efficient photocatalysts. Among them, Ag₂CrO₄ is an important one for its strong optical absorption coefficient in visible-light region as well as narrow band gap. However, the photocatalytic activity of Ag₂CrO₄ is usually weakened by photocorrosion (Yu et al. 2014a, b, 2016; Putri et al. 2015; Komtchou et al. 2016) and the recombining of photogenerated electrons and holes. Researchers find that it can be improved by using some two-dimensional materials. For example, Shang et al. have reported that g-C₃N₄ could increase the photocatalytic efficiency of Ag₂CrO₄ (Shang et al. 2017).

X.-f. Wu (✉) · Z.-h. Zhao · Y. Sun · H. Li · C.-x. Zhang ·
Y.-j. Wang · Y. Liu · Y.-d. Wang · X.-y. Yang · X.-d. Gong
School of Materials Science and Engineering, Hebei Provincial
Key Laboratory of Traffic Engineering Materials, Shijiazhuang
Tiedao University, Shijiazhuang 050043, China
e-mail: wuxiangfeng@stdu.edu.cn

Moreover, Xu et al. have showed that graphene could also improve the organic pollutant degradation of Ag_2CrO_4 (Xu et al. 2015).

Moreover, recent reports show that boron nitride (BN) can enhance the photocatalytic properties of many Ag-based photocatalysts, such as Ag_3VO_4 (Lv et al. 2016), AgI (Choi et al. 2015), and Ag_2PO_4 (Song et al. 2014). As is well-known, few layer boron nitride nanosheets (FBNNS), which can be prepared from BN, possess excellent optical properties, thermal, chemical stability, and high specific surface area (Marsh et al. 2015; Li et al. 2013). However, as far as we have known, there were no reports for using FBNNS to improve the photocatalytic properties of pure Ag_2CrO_4 nanoparticles.

In this work, the $\text{Ag}_2\text{CrO}_4/\text{FBNNS}$ hybrids with various usage amounts of FBNNS were prepared via in situ precipitation method. The photocatalytic activities of the as-prepared hybrids were evaluated by degradation of rhodamine B (RhB) solution under the visible light. Experimental results indicated that FBNNS could obviously improve the photocatalytic activities of pure Ag_2CrO_4 and the possible photocatalytic mechanism was also proposed.

Experimental section

Materials

FBNNS were prepared basing on our previous report (Wu et al. 2017). Potassium chromate (K_2CrO_4), silver nitrate (AgNO_3), and RhB were purchased from Sinopharm Chemical Reagent Co., Ltd., China. All the chemicals were analytical grade.

Preparation of the $\text{Ag}_2\text{CrO}_4/\text{FBNNS}$ hybrids

Firstly, a certain amount of FBNNS (0, 2, 6, 10, or 14 wt% basing on the weight of K_2CrO_4) was stirred with 40 mL H_2O for 30 min. Subsequently, 20 mL 0.05 mmol/mL AgNO_3 solution and 40 mL 0.0125 mmol/mL K_2CrO_4 solution were slowly added into the above mixture, respectively. Finally, the obtained precipitate was fully washed by using distilled water and dried at 50 °C for 6 h. According to the usage amount of FBNNS, the as-prepared $\text{Ag}_2\text{CrO}_4/\text{FBNNS}$ hybrids were labeled as $\text{Ag}_2\text{CrO}_4/\text{FBNNS}$ -2 wt%,

$\text{Ag}_2\text{CrO}_4/\text{FBNNS}$ -6 wt%, $\text{Ag}_2\text{CrO}_4/\text{FBNNS}$ -10 wt%, or $\text{Ag}_2\text{CrO}_4/\text{FBNNS}$ -14 wt%, respectively.

Characterization

The X-ray diffraction (XRD) patterns of the as-prepared samples were measured by X-ray diffraction (XRD, Model: D8ADVANCE, Bruker Co., Germany) with Cu-K α radiation. The UV-visible absorbance spectra of RhB were measured by a UV-visible spectrophotometer (Model: UV-722N, Shanghai Precision Instrument Co., Ltd., China). The solid state UV-vis diffuse reflectance spectra of the samples were obtained by using a UV/VIS/NIR spectrometer (DRS, Model: U-4100, Shimadzu Co., Japan) equipped with a diffuse reflectance accessory. The morphologies of the products were characterized by a transmission electrical microscope (TEM, Model: JEM-2100, JEOL Co., Japan) with an accelerating voltage of 120 kV.

Measurements of photocatalytic activity and electrochemical performances

The photocatalytic activities of the as-prepared $\text{Ag}_2\text{CrO}_4/\text{FBNNS}$ hybrids were evaluated by degradation of RhB under visible light ($\lambda > 420$ nm). A 300-W Xe lamp was adopted as the light source with a 420-nm cutoff filter to provide visible-light irradiation. For degradation of RhB, 50 mg of the as-prepared hybrids were added into 150 mL RhB solution with an initial concentration of 10 mg/L. Before the illumination, the solution was stirred for 1 h in the dark to reach the adsorption-desorption equilibrium between the photocatalyst and RhB. Moreover, at 30 min interval, 4 mL of the suspension was collected and centrifuged to remove the photocatalyst. Then, the concentration of RhB was detected by a UV-vis spectrometer at the characteristic band of 553 nm. The photocatalytic decomposition kinetics was also investigated, and the Langmuir-Hinshelwood model was arranged as the following:

$$\ln(C/C_0) = kt$$

where C_0 and C are the adsorption equilibrium and RhB concentration at reaction time t , respectively. Moreover, k is the apparent reaction rate constant.

Electrochemical measurements were performed on an electrochemical workstation (Model: CHI660E, Shanghai Chenhua Co., China) by using a standard three-

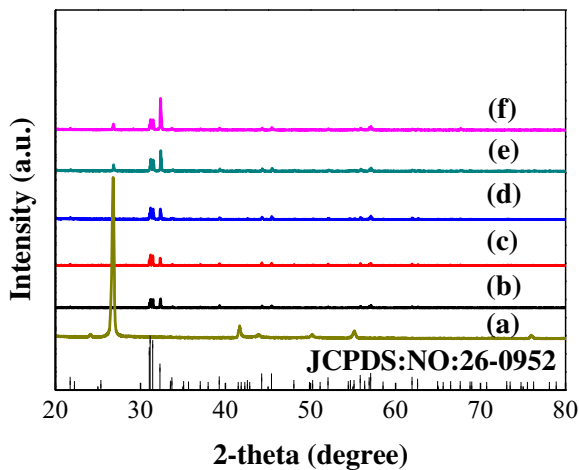


Fig. 1 XRD patterns of the as-prepared hybrids: pure FBNS (a), pure Ag_2CrO_4 (b), $\text{Ag}_2\text{CrO}_4/\text{FBNS}$ -2 wt% (c), $\text{Ag}_2\text{CrO}_4/\text{FBNS}$ -6 wt% (d), $\text{Ag}_2\text{CrO}_4/\text{FBNS}$ -10 wt% (e), and $\text{Ag}_2\text{CrO}_4/\text{FBNS}$ -14 wt% (f)

electrode cell with a working electrode, a platinum wire as counter electrode, and a standard Ag/AgCl in saturated

KCl as reference electrode, respectively. The working electrodes were prepared by dip-coating as follows: 4 mg of the as-prepared photocatalyst was dispersed in 760 μL deionized water, 40 μL ethyl alcohol, and 20 μL nafion membrane solution to produce a suspension, which was then dip-coated onto the glass carbon electrode. The electrochemical impedance spectroscopies (EIS) were carried out at the open circuit potential within a frequency range from 0.01 to 10^5 Hz. In addition, 40 mL 0.5 M KNO_3 solution was used in the experiments containing 0.1 M KCl as an electrolyte.

Results and discussion

XRD analysis

XRD patterns of pure Ag_2CrO_4 and the as-prepared $\text{Ag}_2\text{CrO}_4/\text{FBNS}$ hybrids with various mass fractions of FBNS are shown in Fig. 1. It is seen in Fig. 1a that

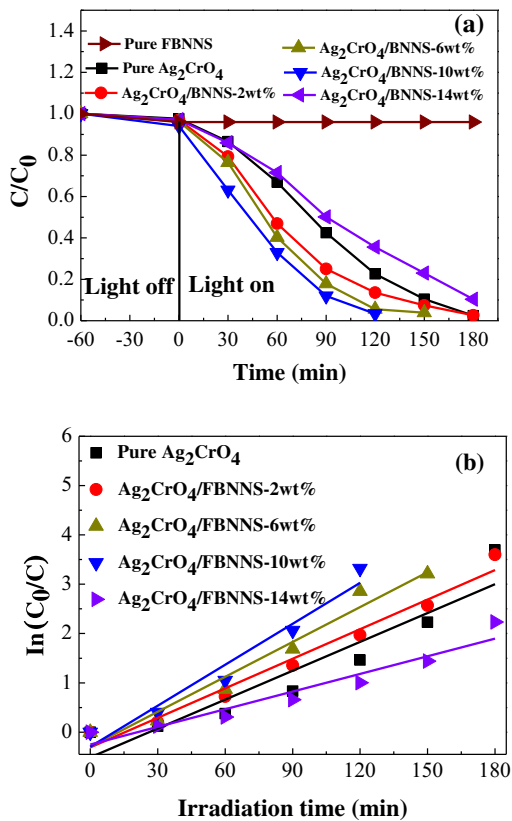
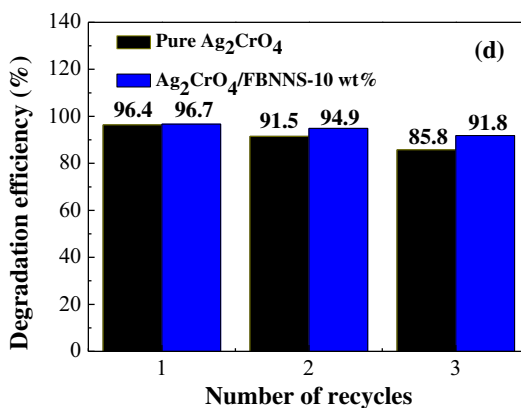
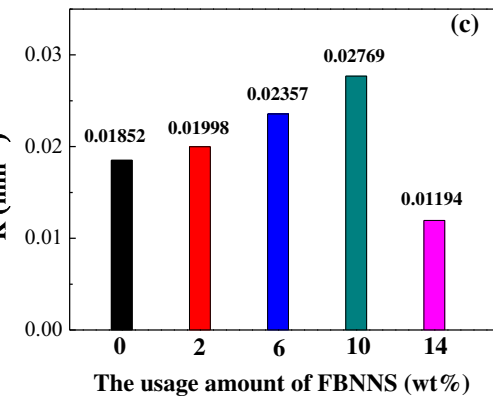
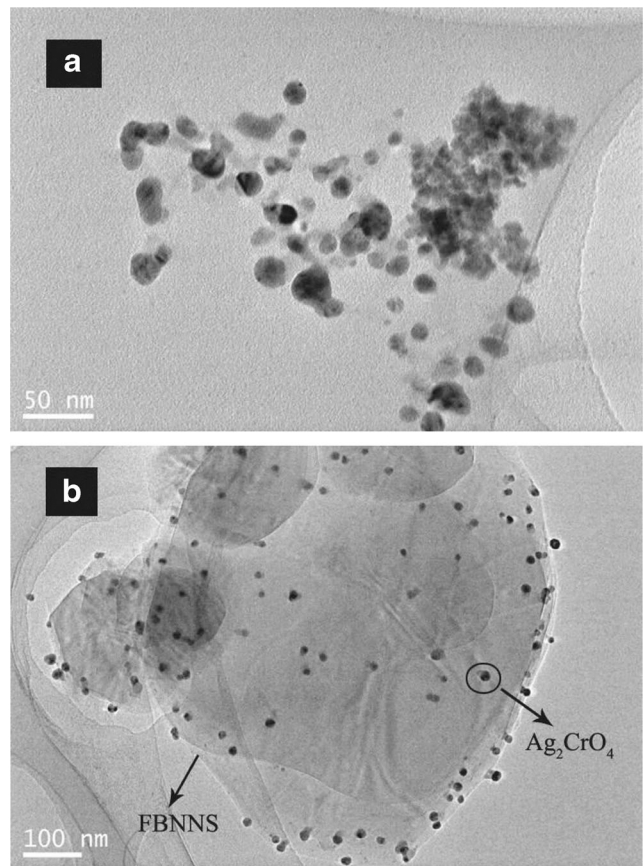


Fig. 2 RhB concentration versus visible-light irradiation time of the as-prepared samples (a). Kinetic linear simulation curves of the as-prepared samples (b). Rate constants κ of as-prepared samples



under the irradiation of visible light ($\lambda > 420$ nm) (c). Cycling runs of pure Ag_2CrO_4 and as-prepared $\text{Ag}_2\text{CrO}_4/\text{FBNS}$ -10 wt% samples (d)

Fig. 3 TEM images of pure Ag_2CrO_4 (a). The as-prepared $\text{Ag}_2\text{CrO}_4/\text{FBNNS}$ -10 wt% hybrids (b)



the diffraction peak at 26.4° was corresponded to (002) plane of FBNS according to JCPDS No. 34-0421 (Fan et al. 2016). Moreover, in Fig. 1b–f, other peaks, especially that typical one at 32.4° , of the as-prepared $\text{Ag}_2\text{CrO}_4/\text{FBNNS}$ samples could be attributed to Ag_2CrO_4 according to JCPDS No. 26-0952. These peaks were also in accord with previous report (Silva et al. 2016). It indicated that FBNS did not change the structure of pure Ag_2CrO_4 nanoparticles.

RhB was chosen as the target pollutant to characterize the photocatalytic activity of pure Ag_2CrO_4 and the as-prepared $\text{Ag}_2\text{CrO}_4/\text{FBNNS}$ hybrids under the visible light. It is seen in Fig. 2a that pure FBNS had no effects on degradation of RhB solution. However, the as-prepared $\text{Ag}_2\text{CrO}_4/\text{FBNNS}$ samples possessed better photocatalytic active than that of pure Ag_2CrO_4 . Moreover, it could be seen that the usage amount of FBNS obviously affected the photocatalytic properties of the as-prepared hybrids. It was first increased and then decreased with increasing the usage amount of the as-prepared samples. When the usage amount of FBNS

was 10 wt%, in 120 min, the as-prepared composites exhibited the highest photocatalytic activity of 96.7%. This was obviously higher than 75% of pure Ag_2CrO_4 . These results might be caused by fewer usage amount of FBNS that could improve the photocatalytic properties of pure Ag_2CrO_4 particles. However, excess amount of FBNS might be impurities and hindered the light absorption of Ag_2CrO_4 , restricting the improvement of photocatalytic activity.

The reaction rate k was also investigated by fitting the first-order kinetic (Ahmed et al. 2016). It is seen in Fig. 2b, c that the k of the as-prepared $\text{Ag}_2\text{CrO}_4/\text{FBNNS}$ -10 wt% was 1.5 times than that of pure Ag_2CrO_4 . In addition, the k of the as-prepared $\text{Ag}_2\text{CrO}_4/\text{FBNNS}$ composites was first increased and then decreased with increasing the usage amount of FBNS. This result is similar with that of Fig. 2a.

In Fig. 2d, the degradation efficiency of pure Ag_2CrO_4 nanoparticles was decreased by 10.6% from 96.4 to 85.8% after it was circulated for three times. However, for the as-prepared $\text{Ag}_2\text{CrO}_4/\text{FBNNS}$ -

10 wt% sample, it was decreased by 4.9% from 96.7 to 91.8%. This indicated that the as-prepared hybrids were more stable than that of pure Ag_2CrO_4 during the photocatalytic process. The possible reason might be that the photoexcited electrons of Ag_2CrO_4 were incorporated into the FBNS nanosheets, which was in favor of existing of the photogenerated electron-hole pairs.

TEM analysis

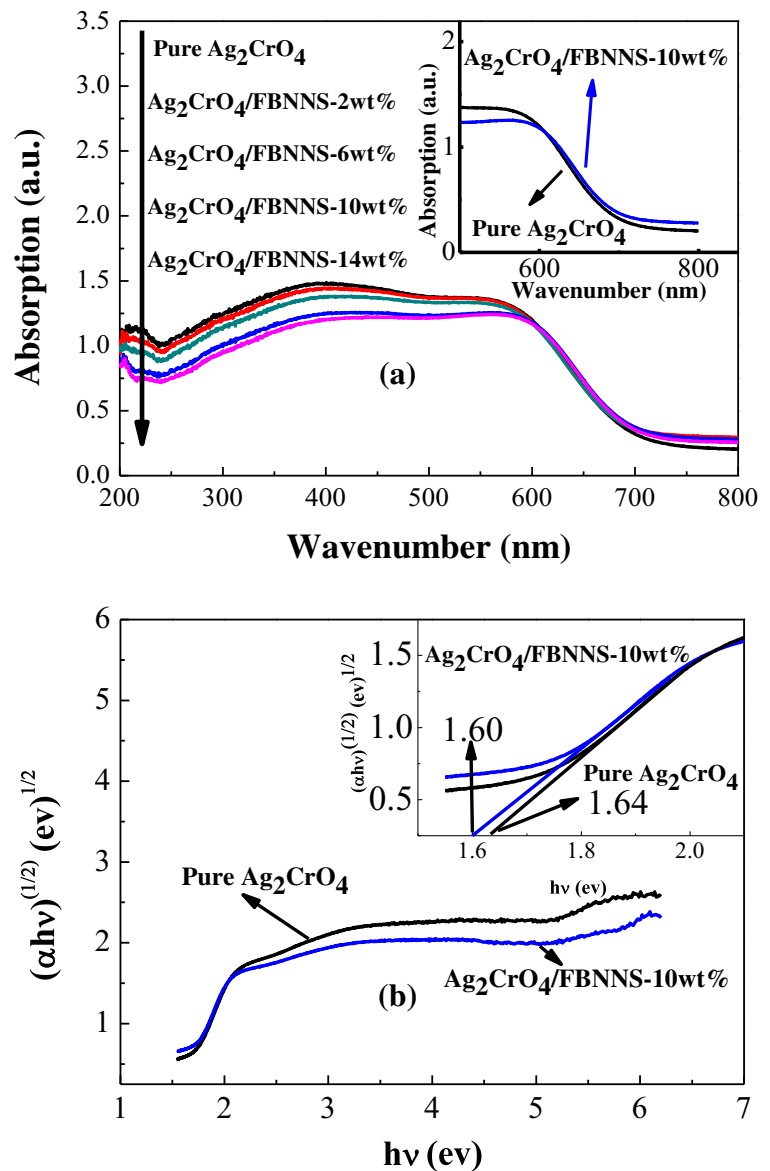
The morphologies of Ag_2CrO_4 nanoparticles and the as-prepared $\text{Ag}_2\text{CrO}_4/\text{FBNS}$ -10 wt% hybrids are shown

in Fig. 3. It could be observed that the average size of Ag_2CrO_4 particles was about 20 nm, as is shown in Fig. 3a. They were well dispersed on the surfaces of the FBNS, as is shown in Fig. 3b. This result revealed that the Ag_2CrO_4 nanoparticles might couple with FBNS through physisorption, electrostatic binding, or charge transfer interactions.

UV-vis diffuse reflectance spectra analysis

Figure 4a shows that all the samples displayed a sharp absorption in the range of 600–750 nm.

Fig. 4 UV-vis diffuse reflectance spectra of pure Ag_2CrO_4 and the as-prepared hybrids (a). The plots of $(\alpha h\nu)^{1/2}$ versus $(h\nu)$ for the pure Ag_2CrO_4 and the as-prepared $\text{Ag}_2\text{CrO}_4/\text{FBNS}$ -10wt% samples (b)



Moreover, the absorption plots of the as-prepared $\text{Ag}_2\text{CrO}_4/\text{FBNNS}$ -10 wt% samples exhibited a slight red-shift compared to pure Ag_2CrO_4 , as shown as the illustration in Fig. 4a. This result indicated that the band gap of the as-prepared $\text{Ag}_2\text{CrO}_4/\text{FBNNS}$ hybrids was slightly narrow than that of pure Ag_2CrO_4 sample.

Figure 4b shows the plot of $(\alpha h\nu)^{1/2}$ versus photon energy ($h\nu$) for pure Ag_2CrO_4 and the as-prepared composites. An enlarged image of the as-prepared $\text{Ag}_2\text{CrO}_4/\text{FBNNS}$ -10 wt% nanocomposites, pure Ag_2CrO_4 , and the band gap energy was shown in the top right corner. It could be seen that the band gap energy of the as-prepared $\text{Ag}_2\text{CrO}_4/\text{FBNNS}$ -10 wt% was 1.60 eV, which was lower than 1.64 eV of pure Ag_2CrO_4 . This result indicated that FBNNS could slightly reduce the band gap energy of pure Ag_2CrO_4 .

EIS analyses

EIS is usually adopted to discuss the charge transfer phenomena at the interfaces of semiconductor photoelectrodes (You et al. 2016). It could be observed in Fig. 5 that the impedance semicircle size of the pure Ag_2CrO_4 sample and the as-prepared $\text{Ag}_2\text{CrO}_4/\text{FBNNS}$ -10 wt% hybrids was the biggest and smallest, respectively. This phenomenon indicated that the as-prepared $\text{Ag}_2\text{CrO}_4/\text{FBNNS}$ hybrids, especially the sample of $\text{Ag}_2\text{CrO}_4/\text{FBNNS}$ -10 wt%, could promote the separation efficiency of electron and hole compared with pure Ag_2CrO_4 . That was to say, the as-prepared $\text{Ag}_2\text{CrO}_4/\text{FBNNS}$ hybrids,

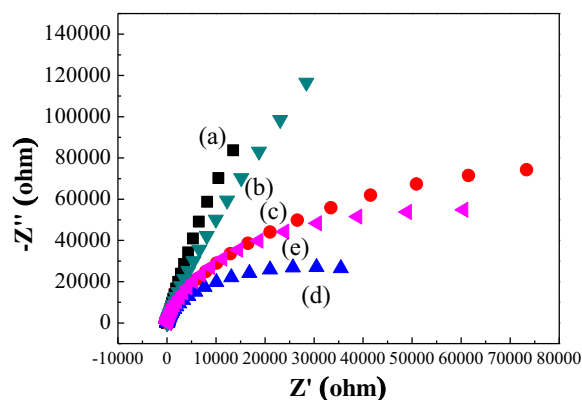


Fig. 5 EIS spectra of pure Ag_2CrO_4 (a), $\text{Ag}_2\text{CrO}_4/\text{FBNNS}$ -2 wt% (b), $\text{Ag}_2\text{CrO}_4/\text{FBNNS}$ -6 wt% (c), $\text{Ag}_2\text{CrO}_4/\text{FBNNS}$ -10 wt% (d), and $\text{Ag}_2\text{CrO}_4/\text{FBNNS}$ -14 wt% (e)

especially the sample of $\text{Ag}_2\text{CrO}_4/\text{FBNNS}$ -10 wt%, possessed faster charge transfer and better photocatalytic performance than that of pure Ag_2CrO_4 . This result was in keeping with that of Fig. 2a.

The possible mechanism of photocatalytic activity

In order to further explore the photocatalytic mechanism of the as-prepared $\text{Ag}_2\text{CrO}_4/\text{FBNNS}$ -10 wt% hybrids. The main active species (holes and hydroxyl scavenger) for the degradation of RhB were assessed by the trapping experiments. As is shown in Fig. 6, the degradation efficiency of RhB was slightly decreased by addition of tertiary butanol (t-BuOH, a hydroxyl radical scavenger) (Xu et al. 2016), while it was remarkably decreased by addition of ethylene diamine tetraacetic acid (EDTA, hole scavenger) (Xing et al. 2015). This result revealed that holes were the main active species during the photocatalytic process.

Based on the above results, the possible charge transfer schematic of the degradation of RhB under visible light for the as-prepared $\text{Ag}_2\text{CrO}_4/\text{FBNNS}$ -10 wt% hybrids is proposed in Fig. 7. It could be seen that the electrons of Ag_2CrO_4 nanoparticles at Valence Band (VB) were excited and transferred to Conduction Band (CB) under visible-light irradiation. The holes were left in the VB of Ag_2CrO_4 . The excited electrons in the CB of Ag_2CrO_4 could transfer to the surfaces of FBNNS due to the interfacial interaction between Ag_2CrO_4 and FBNNS. This effort could suppress the recombination of photogenerated electrons

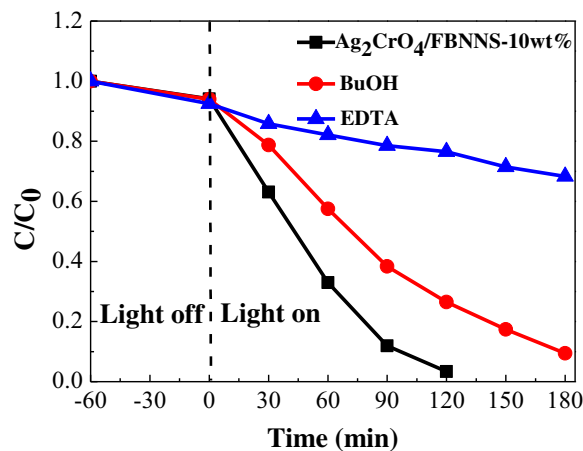
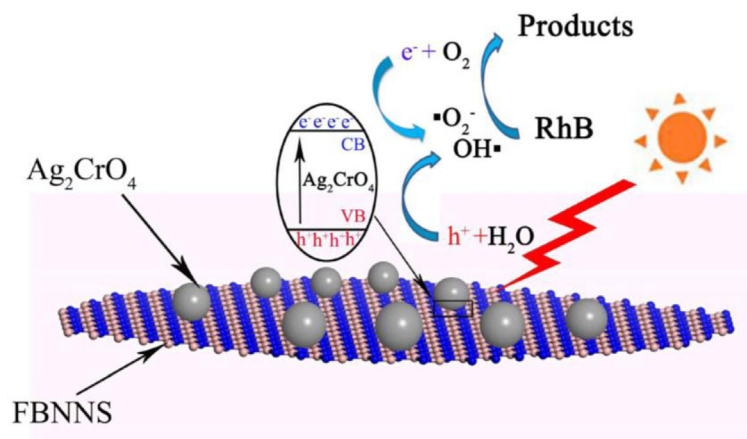


Fig. 6 Photocatalytic degradation of RhB with various scavengers in the presence of the as-prepared $\text{Ag}_2\text{CrO}_4/\text{FBNNS}$ -10 wt% hybrids

Fig. 7 Possible charge transfer schematic for degradation of RhB under visible light



and holes and enhance the photocatalytic activity. At the same time, the excited electrons on the surfaces of FBNNS could be generated to form $\cdot\text{O}_2^-$ with oxygen. Moreover, the excited holes in the Ag_2CrO_4 could form $\text{OH}\cdot$ with H_2O . Finally, the superoxide radical ($\cdot\text{O}_2^-$) and holes (h^+) could oxidize RhB into H_2O and CO_2 during the photocatalytic reaction.

Conclusions

In summary, the $\text{Ag}_2\text{CrO}_4/\text{FBNNS}$ hybrids were prepared via in situ precipitation method. The experimental results showed that the average size of Ag_2CrO_4 particles was about 20 nm and the as-prepared particles were well dispersed on the surfaces of FBNNS. Moreover, the usage amount of FBNNS played an important role on degradation efficiency of the samples. It was first increased and then decreased with increasing the usage amount of the as-prepared samples. When the usage amount of FBNNS was 10 wt%, in 120 min, the composites exhibited highest photocatalytic activity of 96.7%, which was higher than 75% of pure Ag_2CrO_4 . FBNNS could decrease the band gap energy of pure Ag_2CrO_4 , and that of the as-prepared $\text{Ag}_2\text{CrO}_4/\text{FBNNS}$ -10 wt% samples was 1.61 eV. In addition, the holes played mainly active effects during the photocatalytic reaction process. This work could provide potential application in solving the organic pollutant and possess reference values for related works.

Compliance with ethical standards

Funding This study was funded by the Youth Science and Technology Foundation of Higher Education Institutions of Hebei Province, China (grant number Q2012111), and Natural Science Foundation of Hebei Province, China (grant number E2013210011).

Conflict of interest The authors declare that they have no conflict of interest.

References

- Ahmed G, Hanif M, Zhao L, Hussain M, Khan J, Liu Z (2016) Defect engineering of ZnO nanoparticles by graphene oxide leading to enhanced visible light photocatalysis. *J Mol Catal A-Chem* 425:310–321
- Cao W, Chen L, Qi Z (2015) Microwave-assisted synthesis of $\text{Ag}/\text{Ag}_2\text{SO}_4/\text{ZnO}$ nanostructures for efficient visible-light-driven photocatalysis. *J Mol Catal A-Chem* 401:81–89
- Choi J, Reddy DA, Kim TK (2015) Enhanced photocatalytic activity and anti-photocorrosion of AgI nanostructures by coupling with graphene-analogue boron nitride nanosheets. *Ceram Int* 41:13793–13803
- Fan D, Feng J, Liu J, Gao T, Ye ZM (2016) Chen, X. Lv, hexagonal boron nitride nanosheets exfoliated by sodium hypochlorite ball mill and their potential application in catalysis. *Ceram Int* 42:7155–7163
- Komtchou S, Dirany A, Drogui P, Delean N, El Khakani MA, Robert D, Lafrance P (2016) Degradation of atrazine in aqueous solution with electrophotocatalytic process using TiO_2 -x photoanode. *Chemosphere* 157:79
- Li X, Hao X, Zhao M, Wu Y, Yang J, Tian Y, Qian G (2013) Exfoliation of hexagonal boron nitride by molten hydroxides. *Adv Mater* 25:2200–2204

- Lv X, Wang J, Yan Z, Jiang D, Liu J (2016) Design of 3D h-BN architecture as Ag_3VO_4 enhanced photocatalysis stabilizer and promoter. *J Mol Catal A-Chem* 418–419:46–153
- Mali SS, Shim CS, Hong CK (2015) Highly porous zinc stannate (Zn_2SnO_4) nanofibers scaffold photoelectrodes for efficient methyl ammonium halide perovskite solar cells. *Sci Rep* 5: 11424
- Marsh KL, Souliman M, Kaner RB (2015) Co-solvent exfoliation and suspension of hexagonal boron nitride. *Chem Commun* 51:187–190
- Peng Y, Qin S, Wang WS, Xu AW (2013) Fabrication of porous Cd-doped ZnO nanorods with enhanced photocatalytic activity and stability. *Cryst Eng Comm* 15:6518–6525
- Pirhashemi M, Habibi-Yangjeh (2016a) A novel ZnO/ Ag_2CrO_4 nanocomposites with n-n heterojunctions as excellent photocatalysts for degradation of different pollutants under visible light. *J Mater Sci-Mater El* 27:4098–4108
- Pirhashemi M, Habibi-Yangjeh (2016b) A ultrasonic-assisted preparation of novel ternary ZnO/ Ag_3VO_4 / Ag_2CrO_4 nanocomposites and their enhanced visible-light activities in degradation of different pollutants. *Solid State Sci* 55:58–68
- Pirhashemi M, Habibi-Yangjeh A (2015) Ternary ZnO/AgBr/ Ag_2CrO_4 nanocomposites with tandem n-n heterojunctions as novel visible-light-driven photocatalysts with excellent activity. *Ceram Int* 41:14383–14393
- Putri LK, Ong WJ, Wei SC, Chai SP (2015) Heteroatom doped graphene in photocatalysis: a review. *Appl Surf Sci* 358:2–14
- Shang Y, Chen X, Liu W, Tan P, Chen H, Wu L, Ma C, Xiong X, Pan J (2017) Photocorrosion inhibition and high-efficiency photoactivity of porous $g\text{-C}_3\text{N}_4$ / Ag_2CrO_4 composites by simple microemulsion-assisted co-precipitation method. *Appl Catal B-Environ* 204:8–88
- Silva GS, Gracia L, Fabbro MT, Serejo Dos Santos LP, Beltran-Mir H, Cordoncillo E, Longo E, Andres J (2016) Theoretical and experimental insight on Ag_2CrO_4 microcrystals: synthesis, characterization, and photoluminescence properties. *Inorg Chem* 55:8961–8970
- Song Y, Xu H, Wang C, Chen J, Yan J, Xu Y, Li Y, Liu C, Li H, Lei Y (2014) Graphene-analogue boron nitride/ Ag_3PO_4 composite for efficient visible-light-driven photocatalysis. *RSC Adv* 4:56853–56862
- Tong H, Ouyang S, Bi Y, Umezawa N, Oshikiri M, Ye J (2012) Nano-photocatalytic materials: nano-photocatalytic materials: possibilities and challenges. *Adv Mater* 24:229–251
- Wandre TM, Gaikwad PN, Tapase AS, Garadkar KM, Vanalakar SA, Lokhande PD, Sasikala R, Hankare PP (2015) Sol-gel synthesized $\text{TiO}_2\text{-CeO}_2$ nanocomposite: an efficient photocatalyst for degradation of methyl orange under sunlight. *J Mater Sci-Mater El* 27:825–833
- Wu X, Zhao ZH, Sun Y, Li H, Zhang C, Wang Y, Zeng SS, Zhang H (2017) Few-layer boron nitride nanosheets: preparation, characterization and application in epoxy resin. *Ceram Int* 43: 2274–2278
- Xing Y, Que W, Yin X, Liu X, Javed HMA, Yang Y, Kong LB (2015) Fabrication of $\text{Bi}_2\text{Sn}_2\text{O}_7\text{-ZnO}$ heterostructures with enhanced photocatalytic activity. *RSC Adv* 5:27576–27583
- Xu D, Cheng B, Cao S, Yu J (2015) Enhanced photocatalytic activity and stability of Z-scheme $\text{Ag}_2\text{CrO}_4\text{-GO}$ composite photocatalysts for organic pollutant degradation. *Appl Catal B-Environ* 164:380–388
- Xu H, Liu L, Song Y, Huang L, Li Y, Chen Z, Zhang Q, Li J (2016) BN nanosheets modified WO_3 photocatalysts for enhancing photocatalytic properties under visible light irradiation. *J Alloy Compd* 660:48–54
- You D, Pan B, Jiang F, Zhou Y, Su W (2016) CdS nanoparticles/ CeO_2 nanorods composite with high-efficiency visible-light-driven photocatalytic activity. *Appl Surf Sci* 363:154–160
- Yu C, Li G, Kumar S, Yang K, Jin R (2014b) Phase transformation synthesis of novel $\text{Ag}_2\text{O}/\text{Ag}_2\text{CO}_3$ heterostructures with high visible light efficiency in photocatalytic degradation of pollutants. *Adv Mater* 26:892–898
- Yu C, Wei L, Zhou W, Chen J, Fan Q, Liu H (2014a) Enhancement of the visible light activity and stability of Ag_2CO_3 , by formation of $\text{Ag}_2\text{O}/\text{Ag}_2\text{CO}_3$, heterojunction. *Appl Surf Sci* 319:312–318
- Yu C, Zhou W, Hong L, Yuan L, Dionysiou DD (2016) Design and fabrication of microsphere photocatalysts for environmental purification and energy conversion. *Chem Eng J* 287:117–129
- Zhao Z, Wang M, Yang T, Fang M, Zhang L, Zhu H, Tang C, Huang Z (2016) In situ co-precipitation for the synthesis of an $\text{Ag}/\text{AgBr}/\text{Bi}_5\text{O}_7\text{I}$ heterojunction for enhanced visible-light photocatalysis. *J Mol Catal A-Chem* 424:8–16